

# Postsunset vortex in equatorial $F$ -region plasma drifts and implications for bottomside spread- $F$

Erhan Kudeki and Santanu Bhattacharyya

Department of Electrical and Computer Engineering  
University of Illinois at Urbana-Champaign

**Abstract.** Recent high-resolution incoherent scatter drift measurements conducted at Jicamarca during solar minimum conditions indicate that a vortical plasma flow pattern accompanies the well known prereversal enhancement events observed in the equatorial  $F$  region. The vortex is centered at  $\sim 250$  km altitude and about 2000–3000 km east of the evening terminator and is characterized by upward and downward flows to the west and to the east and eastward and westward flows on the top and the bottom, respectively. Postsunset bottomside spread- $F$  events are observed to commence in the interior of the vortex in regions of westward plasma drifts. The formation of the vortex implies localized charging of the postsunset bottomside  $F$  region in response to eastward neutral wind driven  $F$  region dynamo action.

## 1. Introduction

The purpose of this paper is to report incoherent scatter radar observations of a vortical flow pattern in equatorial  $F$  region plasma drifts that has been detected during the postsunset time period. Incoherent scatter drift measurements were conducted at the Jicamarca Radio Observatory near Lima, Peru. In section 2 we will present  $F$  region  $\mathbf{E} \times \mathbf{B}$  drift maps constructed with high resolution vertical and zonal drift estimates derived from recently collected Jicamarca radar data. The maps show well-defined vortex patterns centered at  $\sim 250$  km height and a few thousand kilometers east of the evening terminator. The vortex has only been observed on days exhibiting prereversal or postsunset enhancement of vertical  $F$  region drifts [e.g., Kelley, 1989; Fejer, 1991] and therefore it appears to be the two-dimensional flow structure associated with the prereversal enhancement phenomenon. Postsunset vertical shears in zonal  $F$  region drifts inferred from earlier Barium cloud and coherent radar backscatter experiments [e.g., Valenzuela *et al.*, 1980; Kudeki *et al.*, 1981; Tsunoda *et al.*, 1981] as well as altitudinal variations in vertical  $F$  region drifts reported by Pingree and Fejer [1987] also appear to be associated with the observed vortical flows. In addition, Jicamarca observations show that bottomside spread- $F$  layers [e.g., Woodman and LaHoz, 1976] generally develop in the interior of the vortices and extend eastward into the postreversal ionosphere in their wake. The implications of the new Jicamarca observations concerning the electrodynamic and insta-

bilities of the low-latitude evening ionosphere will be discussed in section 3.

## 2. Observations

New data acquisition and signal processing methods in use at Jicamarca since November 1994 have vastly improved the precision and altitudinal coverage of incoherent scatter plasma drift measurements conducted during World Day experiments. Briefly, the pulse-to-pulse correlation method for drift estimation [Woodman and Hagfors, 1969] has been replaced by a spectral domain maximum-likelihood inversion procedure described by Kudeki *et al.* [this issue]. The correlation method provides about 2 m/s precision for line-of-sight drift estimates acquired with 15 km height and 5 min time resolution when SNR (signal to noise ratio) is greater than 1, but the data quality deteriorates rapidly for  $\text{SNR} < 1$ . The precision with the spectral method, by contrast, is about 1 m/s for SNR values as low as  $\sim 0.1$ . As a consequence, useful drift estimates can now be extracted even from weak returns from the low density regions below the  $F$  region ledge in the postsunset period.

In Plates 1–3 we present three examples of  $\mathbf{E} \times \mathbf{B}$  drift maps constructed with drift estimates obtained with the spectral method. All three plates portray  $F$  region drift variations during the evening period. The arrows in the plates represent vector displacement of  $F$  region plasma in the zonal plane over a 10 min time interval. Vertical and zonal displacement components are proportional to the measured vertical and zonal drift velocities obtained with 15 km and 5 min height and time resolutions, respectively. The zonal displacement components have been scaled in such a way that 5 min local time change along the horizontal axis (i.e., one grid spacing) corre-

Copyright 1999 by the American Geophysical Union.

Paper number 1998JA900111.  
0148-0227/99/1998JA900111\$09.00

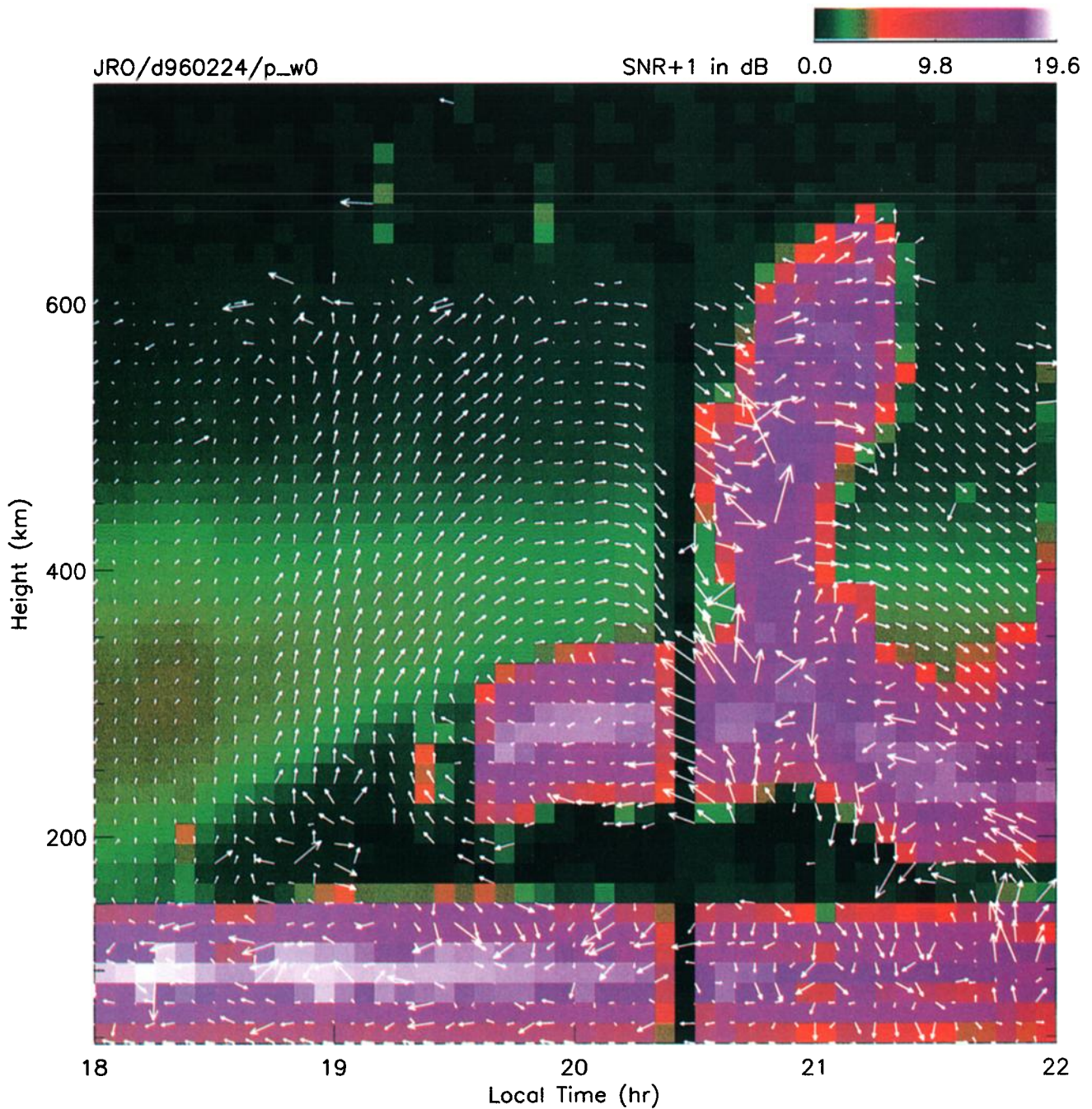


**Plate 1.**  $\mathbf{E} \times \mathbf{B}$  drift and backscattered power map for February 24, 1996 (sunset time 18:32 LT,  $K_p=3-,2+$ ). The vertical black strip at  $\sim 20:30$  LT is due to transmitter failure.



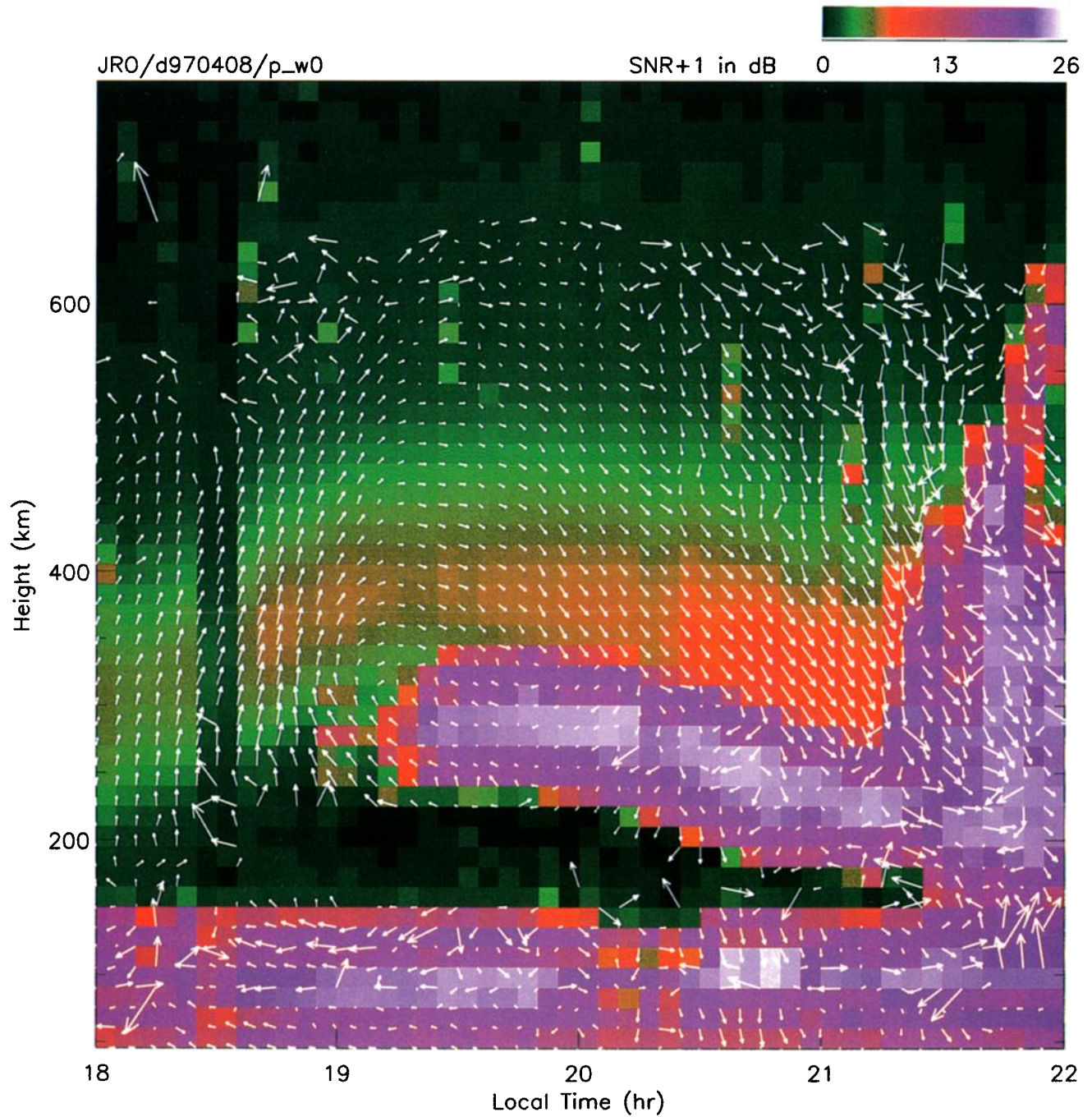
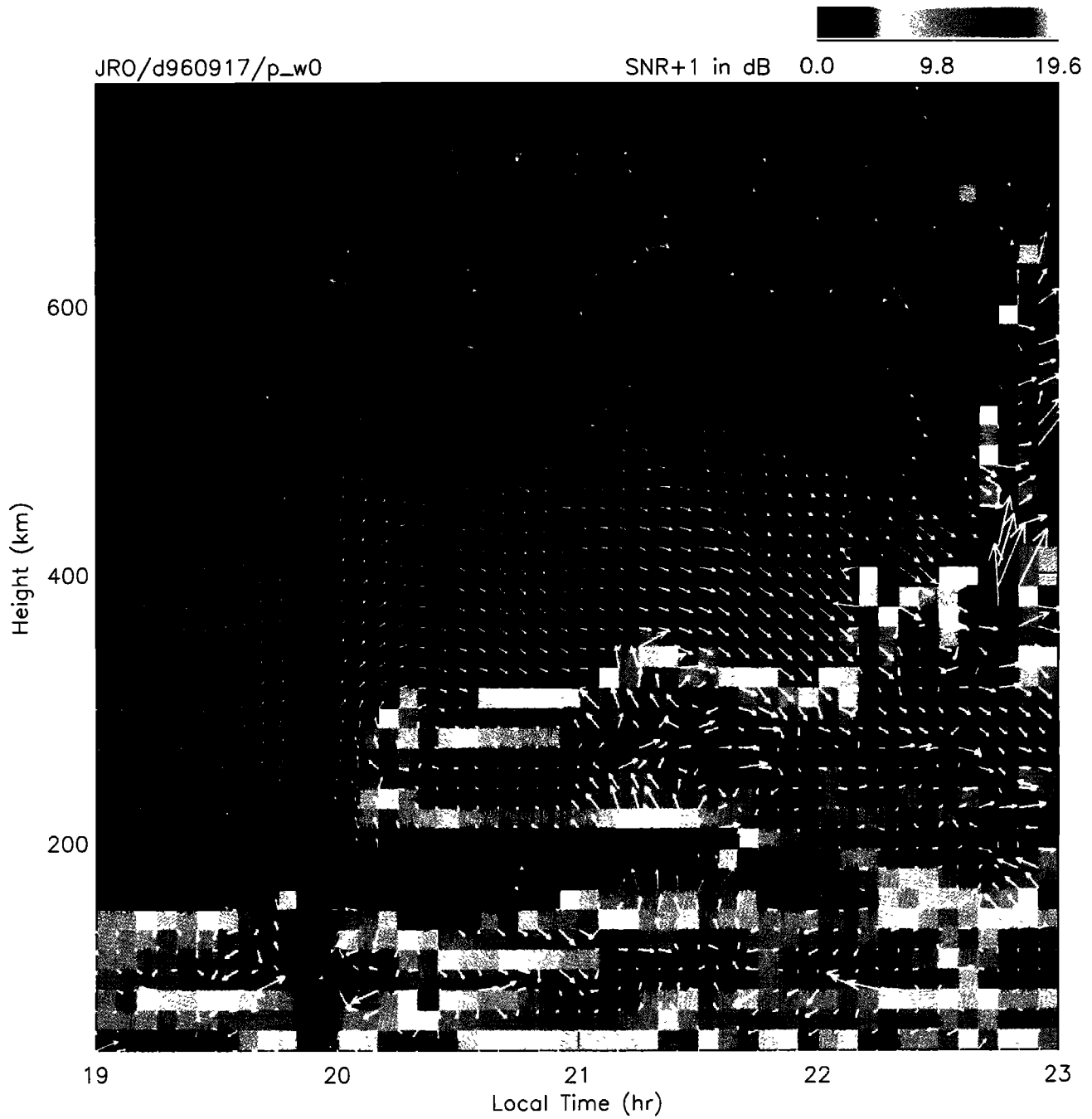


Plate 2.  $E \times B$  drift and backscattered power map for April 8, 1997 (sunset time 18:06 LT,  $K_p=2-,2-$ ).



**Plate 3.**  $E \times B$  drift and backscattered power map for September 17, 1996 (sunset time 18:03 LT,  $K_p=4-,2-$ ). Data quality is poor above  $\sim 500$  km as result of interference from the JRO ionosonde. Also notice a data gap at  $\sim 20:00$  LT.

sponds to  $\sim 139$  km zonal displacement. Arrows pointed to the right indicate eastward plasma motions.

The background color variations in Plates 1-3 depict backscattered signal variations as a function of height and local time. In each plate the color strip on the top shows the correspondence between different colors and SNR+1 expressed in dB. Roughly, black regions correspond to  $\text{SNR} \ll 1$ , greenish tones signify incoherent scatter returns from quiescent ionosphere in thermal equilibrium, and red-to-purple regions indicate coherent backscatter from ionospheric  $E$  and  $F$  region plasma irregularities. Notice that chaotic or noisy flow field signatures in Plates 1-3 are mainly confined to regions returning coherent echoes (red-purple), primarily in portions of spread- $F$  plumes penetrating the  $F$  region peak (see Plates 1 and 2) and the central equatorial electrojet heights. Very large drift estimates obtained within coherent scatter regions exceeding a threshold have been dropped from the plates to minimize clutter. Drift estimates are also absent when the inversion algorithm fails owing to insufficient SNR. However, notice that the flow pattern of the quiescent ionosphere is remarkably well defined even in low SNR regions above and below the  $F$  region peak (the central part of greenish layer), and some drift estimates are available, for the first time in Jicamarca observations, even below the bottomside spread- $F$  layers that develop at  $\sim 250$  km altitude after  $\sim 1930$  LT.

A recurring pattern in  $F$  region flow fields evident in all three plates is a clockwise circulation centered at  $\sim 250$  km altitude and  $\sim 1.5$  hours after the local sunset (1832, 1806, and 1803 LT for Plates 1-3, respectively). In all three plates, but particularly in Plates 1 and 2, the circulation pattern is very clearly defined in the west (primarily upward drifts) as well as at the top and bottom (eastward and westward drifts, respectively). The circulation closes in the east with downward drifts, but the closure region coincides, in all three cases, with bottomside spread- $F$  layers within which the flow pattern seems to be somewhat irregular and harder to resolve than in the stable ionosphere outside the layers. Flow patterns in spread- $F$  layers in fact show some evidence for secondary circulations or vortices; one, in particular, is very clear in Plate 3, between 2100 and 2200 LT. Overall, bottomside spread- $F$  layers are confined to altitudes with predominantly westward plasma flow within the postsunset circulation cell.

Circulation patterns and general features of bottomside spread- $F$  evolution depicted in Plates 1-3 are representative of all recent high-resolution drift observations at Jicamarca conducted on days exhibiting prereversal enhancement. Strong upward drifts in the postsunset period are always followed by a period of about an hour or more exhibiting intense vertical shears in bottomside  $F$  region zonal flows, terminated by an eventual down-drift, possibly followed by the development of secondary circulation cells.

### 3. Discussion

#### 3.1. Interpretation of Drift Maps

$F$  region drift maps presented in section 2 combine the signatures of randomly excited (e.g., spread- $F$  irregularities) as well as deterministic (i.e., local time invariant) flow features. Concerning the spacetime localized random features, the maps generally introduce a "slit camera" distortion effect [e.g., *Woodman and LaHoz*, 1976; *Kelley*, 1989]. As a consequence, the appearance of such features on the maps (altitude-local time plots) may be very different from their actual spatial structure in altitude and longitude. Attempts to interpret the maps as altitude-longitude snapshots often lead to confusion and errors in such cases. However, as far as local time invariant features are concerned, the snapshot interpretation is quite natural and correct. In such an interpretation, one hour increase along the horizontal axis corresponds to  $15^\circ$  or  $\sim 1650$  km of eastward displacement.

The prereversal enhancement is certainly a deterministic feature of the low-latitude electrodynamics. Although the enhancement does not necessarily take place every evening, when it occurs it always occurs at approximately the same local time and its generation mechanism is described by deterministic models [e.g., *Farley et al.*, 1986; *Haerendel and Eccles*, 1992]. Any uncertainty concerning its generation is due to uncertainties in its drivers, for example, zonal thermospheric winds, field-line integrated conductivities, etc. Therefore it is safe to assume that under geomagnetically quiet conditions suitable for its generation, prereversal enhancement will occur uniformly over a wide range of longitudes, and therefore it will be, at least approximately, local time invariant at different longitudes. The snapshot interpretation of Jicamarca drift maps with regard to prereversal enhancement and the associated circulation should then be appropriate. In fact, when in section 2 we were referring to flow features observed at earlier local times as being westward of features observed at later times, we were using that logic.

Using the snapshot interpretation, the implications of Plates 1-3 are the following.

1. The existence of a postsunset vortex in equatorial  $F$  region  $\mathbf{E} \times \mathbf{B}$  drifts centered about 250 km altitude and about 2000-3000 km east of the evening terminator.
2. The vortex is characterized by upward  $\mathbf{E} \times \mathbf{B}$  drifts on the west (prereversal enhancement), eastward and westward drifts on the top and bottom (vertical shear region), and, somewhat less clearly, downward drifts on the east through an unstable region of bottomside spread- $F$ .
3. The vortex is elongated in horizontal direction, with a horizontal dimension of a few thousand kilometers in contrast to a vertical dimension of a few hundred kilometers.

4. Vertical shears near the core region of the vortex can be as intense as  $1\text{-}5\text{ ms}^{-1}/\text{km}$ , corresponding to eddy turnover times of about 1000-200 s.
5. Bottomside spread- $F$  commences within the vortex, and it is generally situated in a layer form just below the altitudes of the most intense shears dominated by westward drifts. The layer extends eastward into the nighttime ionosphere in the wake of the vortex. Vertical drifts within the spread- $F$  layers are generally downward (the closure region of the vortex in the east) but also exhibit irregularities suggesting the possibility of the fragmentation of the vortex in its eastern half into smaller vortices.

We admit here the possibility that some of our inferences regarding the eastern edge of the vortex may be somewhat inaccurate because of slit camera distortion in the spread- $F$  region. Also, it should be noted that our snapshots are representative of solar minimum conditions, and further measurements will be needed to determine how the properties of the vortex change with solar cycle.

Clearly, the most outstanding questions raised by our data concern the morphology and generation of the vortex and possible implications of the vortex for spread- $F$  generation. We will next focus our attention on these questions.

### 3.2. Postsunset Vortex

The observed vortex in  $\mathbf{E} \times \mathbf{B}$  drifts implies a divergent postsunset electric field structure at  $F$  region heights, with electric field vectors pointing toward the core region of the vortex from all directions on the zonal plane. This field geometry requires the presence of negative space charge in the core region. If negative space charge accumulation to the east of the terminator is a consequence of the sunset, then the charged region would be constrained to follow the westward progression of the terminator, inducing a local time invariant prereversal enhancement and vortex structure in the ionosphere at all longitudes as we have assumed in our interpretation of the maps.

Postsunset charging of the bottomside  $F$  region was first described by *Rishbeth* [1971] as a possible cause for the enhancement of eastward  $F$  region plasma drifts after the sunset. Current theories of the prereversal enhancement of vertical drifts also suggest the accumulation of negative space charge in the postsunset ionosphere. In the model by *Farley et al.* [1985], the charging process appears to be driven by eastward thermospheric winds and reduced conductivities to the east of the terminator, and occurs as consequence of the interaction of the equatorial  $F$  region with the field line connected  $E$  layers off the equator. Although the height structure of the resultant charge accumulation is not explicitly discussed in the paper, it appears to us that the described mechanism would give rise to charging

of the field lines with equatorial apex heights near the  $F$  region density maximum. In an alternate model described by *Haerendel and Eccles* [1992] and *Haerendel et al.* [1992], the process is once again driven by eastward thermospheric winds, but charging is attributed to the divergence of upward currents drawn from the equatorial  $E$ -layer. The source of the upward current is described as the divergence in eastward electrojet current in the postsunset  $E$  region. A plasma flow map constructed with computed zonal drifts and assumed vertical drifts (constant in height) presented by *Haerendel et al.* [1992, Figure 13] shows a vortex structure below the main  $F$ -layer very similar to the observed vortices in our data.

The Jicamarca flow maps, which can be regarded as first snapshots of the postsunset vortex, can potentially be instrumental in identifying the correct mechanism for prereversal enhancement and  $F$  region charging. While the observed flow structure can be understood as an electrodynamic response to a westward propagating region of negative space charge, it is also true that the divergence in ionospheric currents driven by the observed fields and thermospheric winds (not directly observed, but of the order of plasma drifts above the vortex) should self consistently account for the propagation of the charged region. Much of the information needed for first principle numerical modeling of the process (none of the existing models resolve the details of the observed flow to the best of our knowledge) is contained in our data.

The theoretical flow map presented by *Haerendel et al.* [1992] suggests a clear closure of the vortex in the east. The closure is also implied by observations since postsunset upward drifts invariably reverse after some time period. Nonetheless, examination of the Jicamarca flow maps reveals that the flow in closure region is quite complicated. There are fluctuations and suggestions of secondary vortices in the data. Part of the complication or uncertainty is undoubtedly due to the onset of spread- $F$  on the eastern side of the vortex and possible breakdown of the assumptions we have been using to interpret the maps. However, it still seems reasonable to us that some of the secondary vortex signatures might be real. We therefore suspect that the vortex may have a natural tendency to fragment at its backside (opposite to propagation direction), which may in turn have some connection with the onset of spread- $F$  within the vortex. Perhaps the dissipation process of space charged region subsequent to prereversal enhancement involves fragmentation to smaller and smaller scales, generating a turbulent wake region behind the westward surging vortex where bottomside spread- $F$  is observed. The absence of subvortices in the results of *Haerendel et al.* [1992] may simply reflect the absence of instability physics in their model. In view of the strong suggestion in our data that postsunset flow structure and bottomside spread- $F$  may be related, we will pursue the discussion of this possibility a little further.

### 3.3. Implications for Spread- $F$ Generation

Let us suppose for a moment that the postsunset vortex indeed has a tendency to break into smaller vortices or eddies as we have suggested above. One of the immediate consequences of such a fragmentation would be the mixing of the sharp vertical density gradient of the bottomside  $F$ -layer. If such a mixing process can generate horizontal density gradients (presumably both eastward and westward directed on different sides of blobs of enhanced density ripped off from higher altitudes), then an interchange instability process driven by the upward  $F$  region current invoked in the theory of *Haerendel et al.* [1992] would cause further structuring of the plasma in the region. We have strong evidence from our data (namely, westward bottomside drifts, as explained below) that the upward current is driven very strongly in the lower half of the vortex occupied by spread- $F$ .

Briefly, upward Pedersen current is proportional to  $E + BU$ , where  $E$  is the upward electric field,  $B$  is geomagnetic flux density, and  $U$  is the eastward zonal wind, all in the reference frame of the Earth. When the driver of the current, electric field  $E + BU$  in the reference frame of the neutrals, is large, the current magnitude is highly sensitive to small variations in plasma density, and, consequently, the potential to set up large polarization fields on density perturbations is very high. The driver is relatively weak on the topside of the vortex and at higher altitudes where eastward drift velocity of the plasma  $-E/B$  and eastward neutral wind  $U$  are approximately equal. However, at bottomside spread- $F$  heights, the observed  $\mathbf{E} \times \mathbf{B}$  drift is primarily westward, i.e.,  $E > 0$ , and therefore  $E + BU$  is large (as needed to maintain vertical current continuity throughout the low-density bottomside region, which, incidentally, may be the simplest explanation of the reason for postsunset charging). Any small-scale structuring imposed on westward density gradients in the bottomside region (caused by mixing, as conjectured above) will then be strongly polarized by the upward current in a manner to cause rapid growth via perturbation  $\mathbf{E} \times \mathbf{B}$  drifts.

What we are describing here (except for some geometrical differences) is the neutral wind driven component of the generalized Rayleigh-Taylor instability [e.g., *Kelley et al.*, 1981] that has been invoked to explain the structuring observed on western walls of spread- $F$  bubbles [e.g., *Tsunoda*, 1983]. What is unusual and relevant in our case is the strength of the driver and its altitudinal localization.

Typical westward drift velocities observed at bottomside spread- $F$  heights are in the 50-100 m/s range. If we assume that eastward neutral wind velocity is also in the same range (reasonable since eastward winds can be as large as 200 m/s higher up), then the relative westward drift velocity  $E/B + U$  of the plasma in the neutral frame would be in the 100-200 m/s range, or even possibly higher. The corresponding 2.5-5 mV/m field in the neutral frame, i.e., the driver  $E + BU$  for interchange

instability on westward gradients, is very large by  $F$  region standards. The driving field of the same instability at bubble heights is significantly smaller (where plasma drift and neutral winds are in the same direction), while the eastward field that drives the  $\mathbf{E} \times \mathbf{B}$  component of the generalized Rayleigh-Taylor instability during the brief ascent phase of  $F$ -layer is only  $\sim 0.5$ -1 mV/m.

So if a fragmentation process of the postsunset vortex suggested by our data (or any other process, for that matter, even if we cannot think of any better candidate than vortex fragmentation) can generate intermediate scale density irregularities within the vortex, then a very strongly driven interchange instability process in the lower half of the vortex would account for the observed bottomside spread- $F$  layers. The process would only be active in the narrow height range where the plasma and neutral flows are opposite (hence the limited thickness of irregular bottomside layers), and, given the strength of its driver, small-scale irregularities responsible for bottomside spread- $F$  radar signatures would develop much earlier than the plume structures excited by the gravitational component of the generalized instability. Eddy turnover times of 1000 s or less deduced from our flow data (item 4 in our summary list in section 3.1) could also be pertinent concerning how fast the conjectured mixing process would proceed to initiate the scenario we have outlined above.

We are not certain whether the outlined scenario is acted out verbatim in the postsunset  $F$  region. However, certainly many of its ingredients are plausible and/or suggested by the observations. The destabilizing potential of counter streaming plasma and neutrals is a certainty, and all the consequences that we can think of are in accord with observations. In view of all these, and the fact that other instability drivers such as vertical drifts (i.e.,  $\mathbf{E} \times \mathbf{B}$  instability) are generally weak and often in the wrong direction (downward) within the irregular layers (item 5), it would be worthwhile to investigate, through modeling work, the inherent stability properties of the postsunset vortex and determine whether some plausible instability mechanism could account for the fragmentation of vortical  $F$  region flow.

Finally, we would like to point out that the stability properties of the vortex may even have implications for the seeding or initiation of plasma bubbles that penetrate the  $F$  region. Spread- $F$  plasma bubbles almost always grow out of bottomside spread- $F$ , and if vortical flows are involved in the dynamics of bottomside spread- $F$ , they could also impact the generation of the bubbles. The large and bulging secondary vortex in Plate 3 (2100-2200 LT) may well be a snapshot of the genesis of a future bubble.

## 4. Summary and Conclusions

We have presented very high quality incoherent scatter  $F$  region drifts data from Jicamarca that provide first snapshots of a postsunset vortex associated with



prereversal enhancement events. We have conjectured that the vortex is a manifestation of negative charging of the postsunset ionosphere in accordance with models proposed to explain the prereversal enhancement phenomenon. Vortex observations are accompanied by bottomside spread- $F$  observations in the westward plasma drift region within the flow structure. Large differential velocity between the plasma and neutrals in this region is almost certainly the cause of fine structuring within the observed spread- $F$  layers. Furthermore, mixing of the bottomside  $F$  region density gradients by vortical flows may be the mechanism responsible for the onset of spread- $F$ .

**Acknowledgments.** We thank Bela Fejer, Ron Woodman, Sergey Fridman, and Dave Hysell for inspiring discussions about our data and their possible implications. We also thank the staff and engineers of the Jicamarca Radio Observatory for their assistance with the observations. The enthusiasm and contributions of Gerardo Vera for Jicamarca World Day observations cannot be overstated. Jicamarca Radio Observatory is operated by the Instituto Geofisico del Peru, with support from the National Science Foundation. This work was supported by the Aeronomy Program, Division of Atmospheric Sciences of the National Science Foundation through grant ATM 94-24361.

Janet G. Luhmann thanks J. Vincent Eccles and another referee for their assistance in evaluating this paper.

## References

- Farley, D. T., E. Bonelli, B. G. Fejer, and M. F. Larsen, The prereversal enhancement of the zonal electric field in the equatorial ionosphere, *J. Geophys. Res.*, *91*, 13723, 1986.
- Fejer, B. G., Low latitude electrodynamic plasma drifts: A review, *J. Atmos. Terr. Phys.*, *53*, 677, 1991.
- Haerendel, G., and J. V. Eccles, The role of the equatorial electrojet in the evening ionosphere, *J. Geophys. Res.*, *97*, 1181, 1992.
- Haerendel, G., J. V. Eccles, and S. Cakir, Theory for modeling the equatorial evening ionosphere and the origin of the shear in the horizontal plasma flow, *J. Geophys. Res.*, *97*, 1209, 1992.
- Kelley, M. C., *The Earth's Ionosphere*, Academic, San Diego, Calif., 1989.
- Kelley, M. C., M. F. Larsen, C. L. Hoz, and J. P. McClure, Gravity wave initiation of equatorial spread F: A case study, *J. Geophys. Res.*, *86*, 9087, 1981.
- Kudeki, E., B. G. Fejer, D. T. Farley, and H. M. Ierkec, Interferometer studies of equatorial F region irregularities and drifts, *Geophys. Res. Lett.*, *8*, 377, 1981.
- Kudeki, E., S. Bhattacharyya, and R. F. Woodman, A new approach in incoherent scatter F region  $E \times B$  drift measurements at Jicamarca, *J. Geophys. Res.*, this issue.
- Pingree, J. E., and B. G. Fejer, On the height variation of equatorial F region vertical plasma drifts, *J. Geophys. Res.*, *92*, 4763, 1987.
- Rishbeth, H., Polarization fields produced by winds in the equatorial F-region, *Planet. Space Sci.*, *19*, 357, 1971.
- Tsunoda, R. T., On the generation and growth of equatorial backscatter plumes, 2, Structuring of the west walls of upwellings, *J. Geophys. Res.*, *88*, 4869-4874, 1983.
- Tsunoda, R. T., R. C. Livingstone, and C. L. Rino, Evidence of a velocity shear in bulk plasma motion associated with the postsunset rise of the equatorial F layer, *Geophys. Res. Lett.*, *8*, 807, 1981.
- Valenzuela, A., G. Haerendel, E. Foppl, H. Kappler, R. F. Woodman, B. G. Fejer, and M. C. Kelley, Barium cloud observations of shear flow in the postsunset equatorial F layer (abstract), *Eos Trans. AGU*, *61*, 315, 1980.
- Woodman, R., and T. Hagfors, Methods for the measurement of vertical ionospheric motions near the magnetic equator by incoherent scattering, *J. Geophys. Res.*, *74*, 1205, 1969.
- Woodman, R. F., and C. LaHoz, Radar observations of F-region equatorial irregularities, *J. Geophys. Res.*, *81*, 5447, 1976.

---

S. Bhattacharyya and E. Kudeki, Department of Electrical and Computer Engineering, 1308 West Main Street, 303 C&SRL, Urbana, IL 61801-2307. (e-kudeki@uiuc.edu)

(Received July 14, 1998; revised November 6, 1998; accepted November 6, 1998.)